Ab Initio Study of the CO_2 Dimer and the CO_2 Ion Complexes $(CO_2)_2^+$ and $(CO_2)_3^+$

Andreas J. Illies, Michael L. McKee,*

Department of Chemistry, Auburn University, Auburn, Alabama 36849

and H. Bernhard Schlegel

Department of Chemisty, Wayne State University, Detroit, Michigan 48202 *(Received: January 14, 1987)*

Ab initio calculations were performed at several levels for neutral CO_2, CO_2 dimer, and the cations $(CO_2)_2^+$ and $(CO_2)_3^+$. At the highest level, a CO_2 neutral dimer of C_{2h} symmetry (staggered side-by-side) is bound by 1.3 kcal/mol, which is 0.2 kcal/mol more stable than a T-shaped dimer (C_{2v} symmetry). The dissociation energy of a $(CO_2)_2^+$ complex of C_{2h} symmetry is calculated to be 16.2 kcal/mol which is 4.4 kcal/mol greater than the dissociation energy of the T-shaped $(CO_2)_2^+$ complex. Due to a smaller amount of spin contamination (spin polarization), the stability of this complex which is characterized by a partial bond between oxygens is overestimated at the [MP4SDQ/6-31G*] level relative to the T-shaped ion complex and CO_2^+ (plus CO_2) which have significant spin contamination. Projecting out the largest spin contaminant at the PMP2/6-31G* level and at the PMP4/3-21G level leads to an estimated decrease in the energy separation between the C_{2h} symmetry complex and the T-shaped complex of 6.3 kcal/mol (relative to the [MP4SDQ/6-31G*] method). Two trimers of $(CO_2)_3^+$ were considered, a cyclic complex (C_{3h}) and a cross-shaped complex (D_{2h}). The more stable $(CO_2)_3^+$ complex (D_{2h}) is bound by 16.0 kcal/mol with respect to monomers. Vibrational frequencies were used to compute entropies of reaction for $(CO_2)_2^+ \rightarrow CO_2 + CO_2^+$ and $(CO_2)_3^+ \rightarrow 2CO_2 + CO_2^+$.

Introduction

The study of gas-phase cluster ions has shown accelerated growth in recent years.[1-7] As examples of interactions which are part electrostatic-part electronic, ion-moleculer clusters provide a unique probe into bond energies which vary from van der Waals attractions to chemical bonds (3-30 kcal/mol). In addition, the study of cluster ions provides insight into the transition from the gas phase to the condensed phase as the cluster size increases.[8] The chemistry of CO_2 cluster ions is of intrest to atmospheric studies of Earth, Mars, and Venus.[9] The enthalpy and entropy of binding have been experimentally determined,[10-14] as well as the mode of decompositon for $(CO_2)_2^+$ [15-19] and $(CO_2)_3^+$.[20]

While no theoretical calculations have been reported for CO_2 ion clusters, several studies have been made on the neutral dimer.[21-24] Interpretations of IR,[25-30] Raman,[31] and molecular beam experiments[32,33] suggest that the structure is either of C_{2v} symmetry (T-shaped)[25-27,32] or of C_{2h} symmetry (staggered side-by-side).[29-31,33] A good summary is given in a CARS study[31] which presents convincing evidence for he nonpolar C_{2h} configuration, in agreement with the majority of theoretical studies.[22-24]

Method

In the following study the program package GAUSSIAN 82 was used throughout.[34] Open-shell species were calculated by using the unrestricted Hartree-Fock (UHF) method for which it is known that the MP perturbation treatment may be slow to converge for large spin contamination.[35] Recent work has shown

(1) Karbarle, P. *Annu. Rev. Phys. Chem.* **1977**, *28*, 445-476.
(2) *Gas Phase Ion Chemistry*; Bowers, M. T., Ed.; Academic: New York, 1979, Vol. 1, 2. 1984, Vol. 3.
(3) Ng, C. Y. In *Advances in Chemical Physics*; Prigogine, I., Rice, S. A., Eds.; Wiley: New York, 1983; Vol. 52, pp 263-362.
(4) Märk, T. D.; Castleman, Jr., A. W. In *Advances in Atomic and Molecular Physics*; Vol. 20, Bates, D. R., Bederson, B., Eds.; Academic: New York, 1985; and references cited therein.
(5) Castleman, A. W.; Keesee, R. G. In *Ion and Electron Swarms*; Lindinger, W., Märk, T. D., Howorka, F., Eds.; Springer Verlag: Berlin, 1984.
(6) Castleman, A. W.; Keesee, R. G. *Chem. Rev.* **1986**, *86*, 589-618.
(7) Celii, F. G.; Janda, K. C. *Chem. Rev.* **1986**, *86*, 507-520.
(8) Castleman, A. W.; Holland, P. M.; Keesee, R. G. *Radiat. Phys. Chem.* **1982**, *20* 57-74.
(9) Meot-Ner (Mautner), M.; Field, F. H. *J. Chem. Phys.* **1977**, *66*, 4527-4531.
(10) Jones, G. G.; Taylor, J. W. *J. Chem. Phys.* **1978**, *68*, 1767-1775.
(11) Rakshit, A. B.; Warneck, P. *Int. J. Mass Spectrom. Ion Phys.* **1980**, *35*, 23-30.
(12) Linn, S. H.; Ng, C. Y. *J. Chem. Phys.* **1981**, *75*, 4921-4926.
(13) Van Koppen, P. A. M.; Kemper, P. R.; Illies, A. J.; Bowers, M. T. *Int. J. Mass Spectrom. Ion Phys.* **1983**, *54*, 263-282.
(14) Keesee, R. G.; Castleman, A. W. *J. Phys. Chem. Ref. Data* **1986**, *15*, 1011-1071.
(15) Stage, A. J.; Shukla, A. K. *Int. J. Mass Spectrom. Ion Phys.* **1980**, *36*, 119-122.
(16) Johnson, M. A.; Alexander, M. L.; Lineberger, W. C. *Chem. Phys. Lett.* **1984**, *112*, 285-290.
(17) Smith, G. P.; Cosby, P. C.; Moseley, J. T. *J. Chem. Phys.* **1977**, *67*, 3818-3830.
(18) Illies, A. J.; Jarrold, M. F.; Wagner-Redeker, W.; Bowers, M. T. *J. Phys. Chem.* **1984**, *88*, 5204-5209 and references cited therein.
(19) Illies, A. J.; Jarrold, M. F.; Bass, L. M.; Bowers, M. T. *J. Am. Chem. Soc.* **1983**, *105*, 5775-5781.
(20) Kim, H.-S.; Jarrold, M. F.; Bowers, M. T. *J. Chem. Phys.* **1986**, *84*, 4882-4887.
(21) Hashimoto, M.; Isobe, T. *Bull. Chem. Soc. Jpn.* **1974**, *47*, 40-44.
(22) Koide, A.; Kihara, T. *Chem. Phys.* **1974**, *5*, 34-48.
(23) MacRury, T. B.; Steele, W. A.; Berne, B. J. *J. Chem. Phys.* **1976**, *64*, 1288-1299.
(24) Brigot, N.; Odiot, S.; Walmsley, S. H.; Whitten, J. L. *Chem. Phys. Lett.* **1977**, *49*, 157-159.
(25) Mannik, L.; Stryland, J. C.; Welsch, H. L. *Can. J. Phys.* **1971**, *49*, 3056-3057.
(26) Fredin, *L.*; Nelander, B.; Ribbegard, G. *J. Mol. Spectrosc.* **1974**, *53*, 410-416.
(27) Lobue, J. M.; Rice, J. K.; Novick, S. E. *Chem. Phys. Lett.* **1984**, *112*, 376-380.
(28) Miller, R. E.; Watts, R. O. *Chem. Phys. Lett.* **1984**, *105*, 409-413.
(29) Gough, T. E.; Miller, R. E.; Scoles, G. *J. Phys. Chem.* **1981**, *85*, 4041-4046.
(30) Guasti, R.; Schettino, V.; Brigot, N. *Chem. Phys.* **1978**, *34*, 391.
(31) Pubanz, G. A.; Maroncelli, M.; Nibler, J. W. *Chem. Phys. Lett.* **1985**, *120*, 313-317.
(32) Novick, S. E.; Davies, P. B.; Dyke, T. R.; Klemperer, W. *J. Am. Chem. Soc.* **1973**, *95*, 8547-8550.
(33) Barton, A. E.; Chablo, A.; Howard, B. J. *Chem. Phys. Lett.* **1979**, *60*, 414-417.
(34) References to basis sets used are collected here. The program package GAUSSIAN 82 was used throughout: Binkley, J. S.; Frisch, M.; Raghavachari, K.; Fluder, E.; Seeger, R.; Pople, J. A. Carnegie-Mellon University. 3-21G basis: Binkley, J. S.; Pople, J. A.; Hehre, W. J. *J. Am. Chem. Soc.* **1980**, *102*, 939. 6-31G basis: Hehre, W. J.; Ditchfield, R.; Pople J. A. *J. Chem. Phys.* **1972**, *56*, 2257. 6-31G* basis: Hariharan, P. C.; Pople, J. A. *Theor. Chim. Acta* **1973**, *28*, 213. Gordon, M. S. *Chem. Phys. Lett.* **1980**, *76*, 163. Francl, M. M.; Pietro, W. J.; Hehre, W. J.; Binkley, J. S.; Gordon, M. S.; DeFrees, D. J.; Pople J. A. *J. Chem. Phys.* **1977**, *77*, 3654. MP2, MP3 correlation treatment: Møller, C.; Plesset M. S. *Phys. Rev.* **1934**, *46*, 618. Pople, J. A.; Binkley, J. S.; Seeger, R. *Int. J. Quantum Chem. Symp.* **1976**, *10*, 1. CPHF: Pople J. A.; Krishnan, R.; Schlegel, H. B.; Binkley, J. S. *Int. J. Quantum Chem. Symp.* **1979**, *13*, 225.

0022-3654/87/2091-3489$01.50/0 © 1987 American Chemical Society

TABLE I: Total Energies (hartrees) for CO_2 and CO_2 Complexes[a]

	CO_2 ($D_{\infty h}$, $^1\Sigma_g^+$)	CO_2^+ ($D_{\infty h}$, $^2\Pi_g$)	CO_2^+ ($D_{\infty h}$, $^2\Pi_u$)	$(CO_2)_2$ (C_{2v}, $^1A_1$)	$(CO_2)_2$ (C_{2h}, ^1A_g)	$(CO_2)_2^+$ (C_{2v}, $^2B_2$)	$(CO_2)_2^+$ (C_{2h}, ^2B_u)	$(CO_2)_3^+$ (D_{2h}, $^2B_{3g}$)	$(CO_2)_3^+$ (C_{3h}, $^2E'$)
				3-21G Geometries					
ZPC(NEV)[b]	7.45 (0)	4.80 (0)	7.14 (0)	15.25 (1)	15.43 (0)	12.82 (0)	12.94 (1)	20.68 (1)	21.21 (2)[c]
3-21G	−186.56126	−186.11763	−185.89536	−373.12698	−373.12818	−372.70618	−372.68997	−559.29067	−559.26195
6-31G	−187.51483	−187.06532	−186.84078	−375.03221	−375.03198	−374.60273	−374.57839	−562.13728	−562.10995
6-31G*	−187.63342	−187.17536	−186.95465	−375.26742	−375.26745	−374.82350	−374.80818	−562.47034	−562.44994
MP2/6-31G	−187.86342	−187.34865	−187.22458	−375.72875	−375.72873	−375.23462	−375.26677	−563.11679	−563.09555
MP3/6-31G	−187.83050	−187.34291	−187.16721	−375.66353	−375.66349	−375.19699	−375.20930		
MP4SDQ/6-31G	−187.85359	−187.36474	−187.22171	−375.70956	−375.70963	−375.24182	−375.25526		
MP2/6-31G*	−188.10542	−187.58078	−187.45092	−376.21264	−376.21314	−375.70528	−375.74122		
PUHF/3-21G	−186.56126	−186.14266	−185.90710			−372.73099	−372.70020		
PMP2/3-21G	−186.90559	−186.42781	−186.28912			−373.36014	−373.38218		
PMP3/3-21G	−186.87470	−186.41503	−186.22997			−373.31745	−373.32410		
PMP4/3-21G	−186.89662	−186.43598	−186.28147			−373.36017	−373.36762		
PUHF/6-31G*	−187.63342	−187.20129				−374.84916	−374.81859		
PMP2/6-31G*	−188.10542	−187.60251				−375.72680	−375.74863		
PMP3/6-31G*	−188.09141	−187.60362							
PMP4/6-31G*	−188.10544	−187.62072							
				6-31G* Geometries					
6-31G*	−187.63418	−187.17659	−186.95705	−375.26978	−375.27023	−374.82693	−374.81062		
MP2/6-31G*	−188.10220	−187.58067	−187.45170	−376.20650	−376.20713	−375.70142	−375.73574		

[a] MP perturbation treatment is made using the frozen-core approximation. [b] Zero point energy (kcal/mol) with the number of negative eignvalues of the force constant matrix given in parentheses. [c] Not a stationary point.

that projecting out the largest spin contaminant (spin annihilation), after the perturbation corrections are made for electron correlation, improves agreement with experiment.[36,37] For that reason, the effect of spin contamination for species in the present study was examined by annihilation of the next highest spin component in the UHF wave function.[36,37]

Two schemes were used to estimate energies at higher levels of theory. In the first scheme, denoted [MP2/6-31G*], the effects of extending the 6-31G basis set to include polarization (6-31G*) and correlation (MP2/6-31G) are added. This approximation has been tested and found to be accurate to within 5 kcal/mol for most closed-shell molecules compared to relative energies obtained when correlation is explicitly included in the larger basis set.[38] However, when relative energies of open-shell species which differ in the amount of spin contamination are compared, the agreement is poorer.[39] The reason is that the energy lowering due to correlation is dependent on the degree of spin contamination. The correlation effect will be smaller for wave functions with significant spin polarization since spatial separation of electrons reduces the need for electrons to correlate their motion. Since the degree of spin contamination (spin polarization) is dependent on the basis set, the correlation effect for one basis set (6-31G) may not be a reasonable estimate for another (6-31G*).[39] An estimate of relative energies using a spin projected wave function is denoted [PMP2/6-31G*] and is expected to avoid the difficulty of basis set dependent spin contamination.

The second method of estimating relative energies,[40] denoted [MP4SDQ/6-31G*] (or [PMP4/6-31G*] using spin-projected wave functions), adds the effect of extending the MP2/6-31G level of theory to include the effect of polarization (MP2/6-31G*) and additional correlation (MP4SDQ/6-31G) as shown in eq 1 where the estimated level is offset with brackets. At the estimated

$$\Delta E[\text{MP4SDQ/6-31G*}] = \Delta E(\text{MP2/6-31G*}) + \Delta E(\text{MP4SDQ/6-31G}) - \Delta E(\text{MP2/6-31G}) \quad (1)$$

[PMP2/6-31G*] and [PMP4/631G*] levels, correlation is estimated starting from the 3-21G basis set rather than the 6-31G basis set.

TABLE II: Calculated Adiabatic Ionization Potential (eV) for the First Two Electronic States of CO_2^+

basis set	$CO_2^+(^2\Pi_g)$	$CO_2^+(^2\Pi_u)$
3-21G Geometry		
3-21G	12.08	18.12
6-31G	12.24	18.35
6-31G*	12.47	18.48
MP2/6-31G	14.01	17.39
MP3/6-31G	12.68	18.05
MP4SDQ/6-31G	13.31	17.20
MP2/6-31G*	14.28	17.82
PUHF/3-21G	11.39	17.81
PMP2/3-21G	13.00	16.78
PMP3/3-21G	12.51	17.55
PMP4/3-21G	12.54	16.74
PUHF/6-31G*	11.76	18.12
PMP2/6-31G*	13.69	17.56
PMP3/6-31G*	13.28	18.19
PMP4/6-31G*	13.19	17.61
[MP2/6-31G*] (+ZPC)	14.24 (14.13)	17.52 (17.51)
[MP4SDQ/6-31G*] (+ZPC)	13.58 (13.47)	17.63 (17.62)
[PMP2/6-31G*] (+ZPC)	13.37 (13.26)	17.45 (17.44)
[PMP4/6-31G*] (+ZPC)	13.23 (13.12)	17.52 (17.51)
6-31G* Geometry		
6-31G*	12.45	18.43
MP2/6-31G* (+ZPC//3-21G)	14.20 (14.09)	17.71 (17.70)
exptl[a]	13.77	17.31

[a] Franklin, J. L.; Dillard, J. G.; Rosenstock, H. M.; Herron, J. T.; Draxl, K.; Field, F. H. "Ionization Potentials, Appearance Potentials, and Heats of Formation of Gaseous Positive Ions"; *Natl. Stand. Ref. Data Ser. (U.S.) Natl. Bur. Stand.* 1969; NSRDS-NBS 26.

Results and Discussion

Total energies at several levels are given in Table I. Geometries of all species except the $(CO_2)_3^+$ ion complexes were optimized at both the 3-21G and the 6-31G* basis set levels. It seems that the 3-21G geometries are better than the 6-31G* geometries judging by energies at the MP2/6-31G*//3-21G and MP2/6-31G*//6-31G* level (Table I). For all species except the $^2\Pi_u$ state of CO_2^+, the use of 3-21G geometries for single-point calculations at the MP2/6-31G* level produces lower total energies than 6-31G* geometries. While adding polarization functions resulted in longer interactions (compared to 3-21G geometries) between CO_2 units (Figure 1), the further addition of correlation

(35) Handy, N. C.; Knowles, P. J.; Somasundram, K. *Theor. Chim. Acta* **1985**, *68*, 87–100. Gill, P. M. W.; Radom, L. *Chem. Phys. Lett.* **1986**, *132*, 16–22.
(36) Sosa, C.; Schlegel, H. B. *Int. J. Quantum Chem.* **1986**, *29*, 1001–1015. Schlegel, H. B. *J. Chem. Phys.* **1986**, *84*, 4530–4534.
(37) Spin projection at the PMP2 and PMP3 levels will be a standard feature of the GAUSSIAN 86 program (to be released).
(38) McKee, M. L.; Lipscomb, W. N. *J. Am. Chem. Soc.* **1981**, *103*, 4673. Nobes, R. H.; Bouma, W. J.; Radom, L. *Chem. Phys. Lett.* **1982**, *89*, 497. McKee, M. L.; Lipscomb, W. N. *Inorg. Chem.* **1985**, *24*, 762.
(39) McKee, M. L. *J. Phys. Chem.* **1986**, *90*, 2335–2340.
(40) For a similar estimation of basis set extension see: Luke, B. T.; McLean, A. D. *J. Phys. Chem.* **1985**, *89*, 4592–4596.

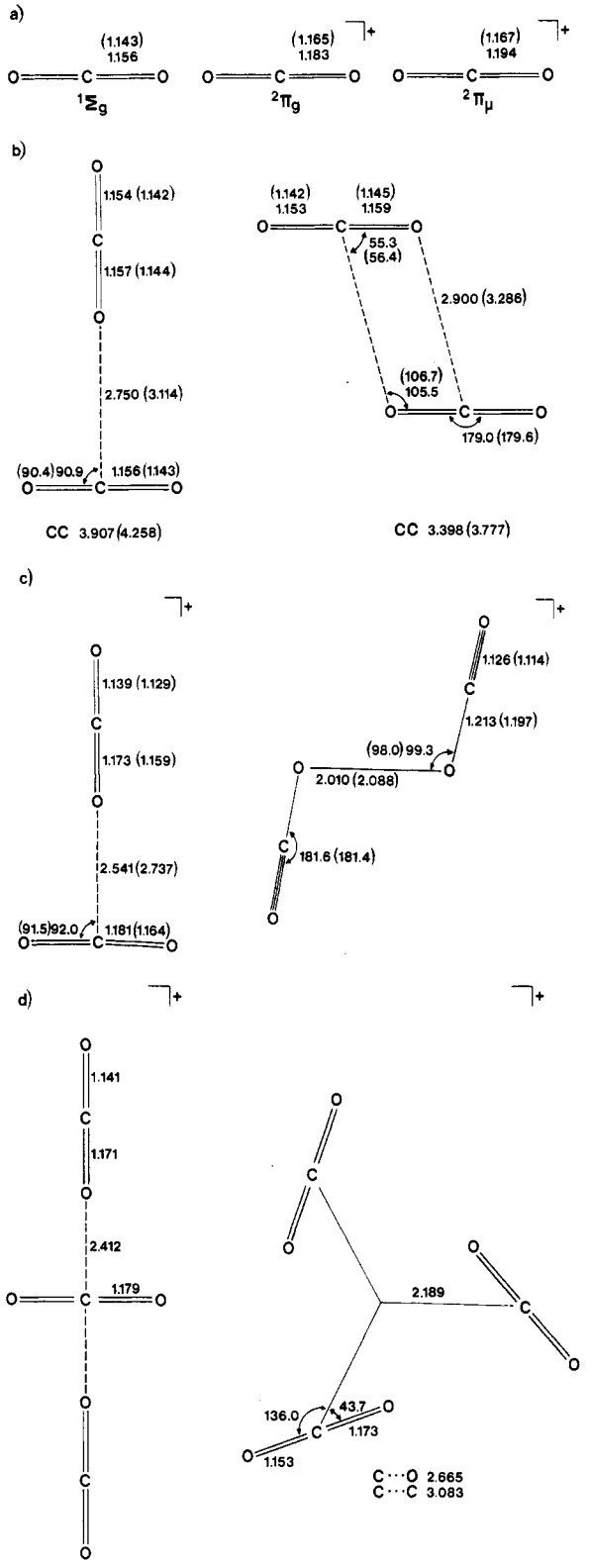

Figure 1. Calculated geometric parameters for various species at the 3-21G and (6-31G*) levels: (a) CO_2 and two states of CO_2^+; (b) two forms of $(CO_2)_2$; (c) two forms of $(CO_2)_2^+$; (d) two forms of $(CO_2)_3^+$.

(i.e., MP2/6-31G*) must favor shorter interactions (compared to 6-31G* geometries). As has been shown for the $(H_2S)_2^+$ complex,[41] the two corrections nearly cancel, leading to good agreement between the 3-21G (optimized) and the MP2/6-31G* (partially optimized) geometries. Unless otherwise indicated, reported energies will be at the 3-21G optimized geometries. The optimized geometries for all the molecules reported in this work are shown in Figure 1.

(41) Fernández, P. F.; Ortiz, J. V.; Walter, E. A. *J. Chem. Phys.* **1986**, *84*, 1653–1658.

TABLE III: Spin-Squared Values (before Projection) for Various Open-Shell Species

	CO_2^+		$(CO_2)_2^+$		$(CO_2)_3^+$	
basis set	$^2\Pi_g$	$^2\Pi_u$	C_{2v}	C_{2h}	D_{2h}	C_{3h}
3-21G	0.99	0.82	0.98	0.81	0.99	0.96
6-31G	1.01	0.82	1.01	0.82	1.01	0.98
6-31G*	0.90	0.82	0.98	0.80	0.98	0.95
MP2/6-31G	0.93	0.78	0.93	0.79	0.93	0.90
MP2/6-31G*	0.90	0.78	0.90	0.77		

TABLE IV: Vibrational Frequencies (cm^{-1}) Calculated at the 3-21G Level for CO_2^+ ($^2\Pi_g$)[a]

linear		nonlinear[b]		obsd[c]	
sym	freq	sym	freq	CO_2^+	CO_2
π_u	−450/859	a_1	466	519	667
σ_u	1194	b_2	1194	1230	1388
σ_g	1230	a_1	1230	1475	2349

[a] The zero-point energy of the $^2\Pi_u$ state of CO_2^+ was estimated by calculating the vibrational frequencies in the C_{2v} point group and doubling the contribution of the lowest frequency (which is degenerate in the linear ion). For the $^2\Pi_g$ state this approximation leads to a zero-point energy of 4.80 kcal/mol. [b] The O=C=O angle is set to 179.99°. [c] Baer, T.; Guyon, P. M. *J. Chem. Phys.* **1986**, *85*, 4765–4778 and references cited therein.

CO_2^+. A single-configurational SCF approach cannot described the wave function symmetry for a degenerate electronic state such as the $^2\Pi_g$ or $^2\Pi_u$ states of CO_2^+. Nevertheless the energy of one component of the electronic state is moderately well reproduced as shown in Table II where energies relative to CO_2 are reported. At the PMP4/6-31G* level, the adiabatic ionization energy for the $^2\Pi_g$ state of CO_2^+ is underestimated by 13.4 kcal/mol (0.58 eV), while the ionization energy for the $^2\Pi_u$ state is overestimated by 6.9 kcal/mol (0.30 eV).

The amount of spin contamination differs between the $^2\Pi_g$ (1.01–0.90) and the $^2\Pi_u$ (0.77–0.82) states of CO_2^+ (Table III). In rough correspondence, the effect of different orders of MP perturbation is much larger for the $^2\Pi_g$ than the $^2\Pi_u$ state (MP2/6-31G through MP4SDQ/6-31G, Table II) when both are compared to neutral CO_2. Projecting out the next higher spin contaminant (PMP2/3-21G − PMP4/3-21G and PMP2/6-31G*) − PMP4/6-31G*) does not improve the rate of convergence. Thus, even higher orders of perturbation may be required for the ionization potential to converge with respect to order of perturbation for the $^2\Pi_g$ state of CO_2^+.

When the vibrational frequencies of the CO_2^+ ionic states were calculated by using analytical second derivatives, an imaginary mode was obtained for one component of the degenerate bending mode (Table IV). This can be traced to the inadequacies of the single determinantal wave function describing the doubly degenerate state of the linear molecule. If a slight distortion of the O=C=O angle is made (179.99°), the electronic degeneracy is lifted and the bending mode in C_{2v} symmetry is found to be 466 cm^{-1}. The zero point energy can then be estimated for linear CO_2^+ by doubling the contribution from the single bending mode. There is little variation between the two methods for the symmetric and antisymmetric C=O stretches.

$(CO_2)_2$. Some doubt exists on the structure of the CO_2 dimer. Experimental and theoretical work can be cited which favor either the T-shaped structure (C_{2v})[21,25-27,32] or the staggered side-by-side structure (C_{2h}).[22-24,29-31,33] Both the structure and the binding of the neutral complex are of interest to experimentalists. A different geometry for the neutral $(CO_2)_2$ complex compared to the ion complex, $(CO_2)_2^+$, might lead to an underestimation of the binding energy of the ion complex by photoionization (PI) methods since the observed excitation of $(CO_2)_2$ may not correspond to the minimum energy structure of $(CO_2)_2^+$.[18] The dissociation energy of $(CO_2)_2$, $E_d(CO_2)_2$, is also required in order to extract the dissociation energy of the complex ($E_d(CO_2)_2^+$) from the photoionization data. The data required in the photoionization

TABLE V: Calculated Dissociation Energy (kcal/mol) for $(CO_2)_2$ and $(CO_2)_2^+$

basis set	$(CO_2)_2$		$(CO_2)_2^+$	
	C_{2v}	C_{2h}	C_{2v}	C_{2h}
	3-21G Geometry			
3-21G	2.80	3.55	17.13	6.95
6-31G	1.60	1.46	14.17	1.10
6-31G*	0.36	0.38	9.24	0.38
MP2/6-31G	1.20	1.19	14.15	34.34
MP3/6-31G	1.59	1.56	14.80	22.53
MP4SDQ/6-31G	1.49	1.54	14.74	23.18
MP2/6-31G*	1.13	1.44	11.98	34.54
PUHF/3-21G			16.99	-2.34
PMP2/3-21G			16.78	30.62
PMP3/3-21G			17.40	21.57
PMP4/3-21G			17.30	21.98
PUHF/6-31G*			9.07	-10.12
PMP2/6-31G*			11.84	25.55
[MP2/6-31G*] (+ZPC)	-0.04 (-0.39)	0.11 (-0.42)	9.22 (8.65)	33.62 (32.93)
[MP4SDQ/6-31G*] (+ZPC)	1.42 (1.07)	1.79 (1.26)	12.57 (12.00)	23.38 (22.69)
[PMP2/6-31G*] (+ZPC)			8.86 (8.29)	22.84 (22.15)
[PMP4/6-31G*] (+ZPC)			12.36 (11.79)	16.90 (16.21)
dipole moment/6-31G*	0.36	0.0		
	6-31G* Geometry			
6-31G*	0.89	1.17	10.24	-0.09
MP2/6-31G* (+ZPC//3-21G)	1.32 (0.98)	1.71 (1.18)	11.64 (11.07)	33.19 (32.50)
dipole moment/6-31G*	0.22	0.0		

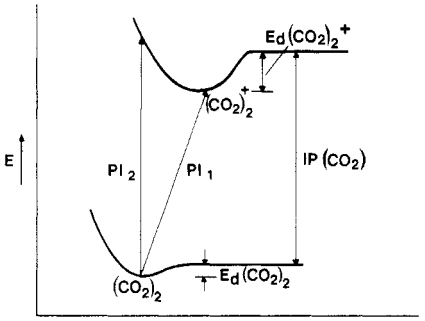

Figure 2. Simplified diagram illustrating the various components needed in a photoionization experiment to obtain the dissociation energy of $(CO_2)_2^+$. If a geometry change occurs between the neutral and charged cluster, the photoionization energy may be too large (PI_2), resulting in an underestimation of the dissociation energy of $(CO_2)_2^+$.

experiment are given in Figure 2. If the geometries of the neutral and charged complexes are significantly different, the desired value, PI_1, may not be observed (due to small Franck–Condon factors) but rather PI_2 is measured where $PI_2 > PI_1$. The dissociation energy of $(CO_2)_2^+$ is given as eq 2. An uncertainty in

$$E_d(CO_2)_2^+ = IP(CO_2) + E_d(CO_2)_2 - PI \qquad (2)$$

$E_d(CO_2)_2$ will lead to an equal uncertainty in $E_d(CO_2)_2^+$ (Figure 2). Also, a large change in the equilibrium geometry of $(CO_2)_2$ and $(CO_2)_2^+$ may lead to an overestimation of the photoionization energy and consequently to an underestimation of the $(CO_2)_2^+$ dissociation energy. Photoionization measurements often lead to a smaller bond dissociation energy compared to equilibrium measurements.[18] In the case of $(CO_2)_2^+$ the former leads to a value of about 12 kcal/mol while the latter leads to a value of about 16 kcal/mol.

Various calculations and empirical schemes for estimating dissociation energies for $(CO_2)_2$ predict a value of 1–2 kcal/mol yielding the staggered side-by-side structure (C_{2h}) more stable than the T-shaped structure (C_{2v}).[22-24] The dissociation energies calculated at various levels are given in the first two columns of Table V. The C_{2h} structure is more stable than the C_{2v} structure at almost all levels. In fact the one calculated imaginary frequency[42] of the C_{2v} structure at the 3-21G level ($15i$ cm^{-1}) corresponds to a motion in the direction of the C_{2h} structure. At the [MP4SDQ/6-31G*] + ZPC level, the dissociation energy of $(CO_2)_2$ is 1.3 kcal/mol and favors the C_{2h} form over the C_{2v} form by 0.2 kcal/mol.

The optimized C–C distance in the C_{2v} structure (Figure 1) is calculated to be 3.907 Å at the 3-21G level (4.258 Å, 6-31G*) while the same parameter in the C_{2h} structure is 3.398 Å (3.777 Å, 6-31G*). This compares to previous calculated C–C separations of 4.1–4.3 Å for the C_{2v} structure and 3.4–3.5 Å for the C_{2h} structure.[24] The persistent preference of the C_{2h} structure over the C_{2v} structure is in agreement with recent experimental evidence.[31] In order to assist infrared studies, the predicted vibration frequencies of the complexes at the 3-21G level are given in Table VI where the new bands due to association are indicated.

$(CO_2)_2^+$. The calculated dissociation energy for $(CO_2)_2^+$ is also given in Table V. The C_{2v} symmetry structure (T-shaped) is less stable than the C_{2h} symmetry structure (slipped side-by-side) by 10.7 kcal/mol at the [MP4SDQ/6-31G*] + ZPC level and by 4.4 kcal/mol at the [PMP4/6-31G*] + ZPC level. Geometric parameters at the 3-21G and 6-31G* levels are given in Figure 1 for both structures. The distortions of the C_{2v} ion complex correspond to a charged CO_2^+ forming the head of the T-shaped structure. The C_{2h} structure contains symmetric CO_2 moieties which are characterized by a short oxygen–oxygen interaction (2.010 Å, 3-21G; 2.088 Å, 6-31G*). The adjacent C–O distances have lengthened to 1.213 Å at the 3-21G level (1.197 Å, 6-31G*) and suggest that the O–O interaction represents a 2-center 3-electron bond. It is known that the stability of some cluster ions, such as $(CO)_2^+$, is greater than expected for ion–dipole interactions and it has been suggested[1] that some sharing of electrons (bonding) by the two molecules must occur.

At the 6-31G*//3-21G level the C_{2h} ion complex is bound by only 0.4 kcal/mol compared to 9.2 kcal/mol for the C_{2v} complex. However, correlation has a dramatic effect on the C_{2h} structure which becomes more stable than the C_{2v} structure. At the 3-21G level the C_{2h} structure has one large imaginary frequency[42] ($2272i$ cm^{-1}) which when reoptimized in the C_s point group using the 3-21G basis, rearranges to the C_{2v} structure which is 10.2 kcal/mol more stable at that level. In order to predict realistic frequencies for the C_{2v} structure one would have to calculate frequencies with a method that gives the correct ordering of energies (i.e., MP2/3-21G or better).[43]

(42) A single imaginary frequency is characteristic of saddle points (transition states) while local minima have all real frequencies. Hehre, W. J.; Radom, L.; Schleyer, P. v. R.; Pople, J. A. *Ab Initio Molecular Orbital Theory*; Wiley: New York, 1986.

(43) Testing for the number of negative eigenvalues of the force constant matrix is important since it allows one to characterize points on the energy hypersurface *at that level*. However, there is no guarantee that the nature of stationary points will be carried over when higher levels of theory are employed.

TABLE VI: Calculated Vibrational Frequencies (cm^{-1}) at the 3-21G Level for $(CO_2)_2$ and $(CO_2)_2^+$ Structures[a]

$(CO_2)_2$				$(CO_2)_2^+$			
C_{2h}		C_{2v}		C_{2v}		C_{2h}	
sym	freq	sym	freq	sym	freq	sym	freq
a_u	43	b_2	15*i*	b_2	40	b_u	2272*i*
b_u	55	b_1	27	b_2	99	a_u	63
a_g	75	a_1	95	b_1	99	a_g	153
a_g	179	b_2	98	a_1	186	b_u	203
b_g	657 (659, CO_2)	b_2	657	a_1	449 (515, CO_2^+)	a_g	438
b_u	661 (659, CO_2)	b_1	658	b_1	584 (515, CO_2^+)	b_g	611
a_u	669 (659, CO_2)	a_1	660	b_2	665 (659, CO_2)	a_u	622
a_g	671 (659, CO_2)	b_1	666	b_1	666 (659, CO_2)	a_g	657
b_u	1426 (1428, CO_2)	a_1	1429	b_2	1012 (1197, CO_2^+)	b_u	822
a_g	1427 (1428, CO_2)	a_1	1433	a_1	1244 (1230, CO_2^+)	a_g	1280
b_u	2465 (2463, CO_2)	b_2	2470	a_1	1427 (1428, CO_2)	b_u	1871
a_g	2466 (2463, CO_2)	a_1	2474	a_1	2500 (2463, CO_2)	a_g	2333

[a] In parentheses are given the frequencies of the unperturbed CO_2 or CO_2^+ modes. The four unlabeled frequencies originate from the association of two molecules. The frequencies for CO_2^+ are from the numerical results in Table IV where the π_u mode is taken as the average of the two bending frequencies. See Table IV for the experimental frequencies of CO_2 and CO_2^+.

Part of the stabilizing effect of correlation on the C_{2h} structure is due to the smaller degree of spin contamination compared to CO_2^+ (plus CO_2) and the C_{2v} ion complex, $(CO_2)_2^+$ (Table II). Accounting for correlation through MP4SDQ/6-31G reduces the stability of the C_{2h} structure compared to the C_{2v} structure at the MP2/6-31G level (Table V), but as shown[39] in the reaction $H^\bullet + C_2H_4 \rightarrow C_2H_5^\bullet$, a 10 kcal/mol error may remain in the barrier at the MP4 level due to different degrees of spin contamination in the transition state and reactants. Binding energies at spin projected levels (Table V) are about the same for the C_{2h} complex at the MP4SDQ/6-31G level compared to the PMP4/3-21G level (23.2 and 22.0 kcal/mol, respectively). However, a much larger difference is found for the MP2/6-31G* level compared to the PMP2/6-31G* (34.5 and 25.6 kcal/mol, respectively). When the results are combined, the binding energy for the C_{2h} complex is reduced from 22.7 kcal/mol at the [MP4SDQ/6-31G*] + ZPC level to 16.2 kcal/mol at the [PMP4/6-31G*] + ZPC level.

In the C_{2h} ion complex, the unpaired spin is located principally on the two adjacent oxygens. A valence bond description would contain a significant contribution from **1** in which the unpaired

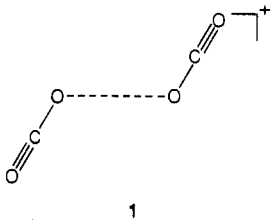

1

electron is in an antibonding O–O orbital. The O–O bond order would then be approximately $^1/_2$ (1 bonding electron pair − $^1/_2$ antibonding electron pair).

A comparison of calculated and experimental thermodynamic values for the $(CO_2)_2^+$ complex is made in Table VII. The small energy difference between the C_{2v} and C_{2h} structures makes it difficult to predict which structure will ultimately be favored in the limit of basis set improvement and more extensive correlation. Thermodynamic properties cannot be calculated for the C_{2h} ion complex due to the qualitative difference in the potential energy surface (and hence in the vibrational frequencies) at the 3-21G level and at higher levels. However, the calculated entropy change at the 3-21G level for the dissociation of the C_{2v} ion complex (Table VII) is in good agreement with experiment.

The calculated vibrational frequencies of the C_{2v} and C_{2h} ion complexes are given in Table VI where each frequency can be assigned to CO_2, CO_2^+, or the association of CO_2 and CO_2^+. These will be useful in calculations using statistical phase space theory which requires the vibrational frequencies of the ion complex. In a recent application to $(CO_2)_2^+$ these frequencies were estimated.[19]

$(CO_2)_3^+$. Two geometries were considered for the $(CO_2)_3^+$ ion complex, one of C_{3h} symmetry and the second of D_{2h} symmetry

TABLE VII: Heat Capacities and Entropies (cal mol^{-1} K^{-1}) at the 3-21G Level[a] and Enthalpies (kcal mol^{-1} at 0 K) Calculated for $(CO_2)_2$, $(CO_2)_2^+$, and $(CO_2)_3^+$

		ΔC_v	ΔS		ΔH	
complex	sym	this work	this work	exptl	this work	exptl
$(CO_2)_2$	C_{2h}	3.78	19.74		1.26	
$(CO_2)_2^+$	C_{2v}	2.87	21.31	19.1[b]	11.8 (12.0)[c]	
	C_{2h}				16.2 (22.2)[c]	15.6[b]
$(CO_2)_3^+$[d]	D_{2h}	6.86	47.90	42.5[e]	16.0	23.0[f]

[a] The heat capacity and entropy for CO_2^+ were calculated by taking finite differences of the analytical first derivatives to determine vibrational frequencies for the linear ion. [b] Reference 14. [c] Estimated at the [PMP4/6-31G*] + ZPC level with the value at the [MP4SDQ/6-31G*] + ZPC level in parentheses. [d] For the reaction $(CO_2)_3^+ \rightarrow 2CO_2 + CO_2^+$. [e] Reference 14. Sum of entropy differences for the first two steps (19.1 + 23.4 cal mol^{-1} K^{-1}). [f] The experimental dissociation energy of CO_2 in the reaction $(CO_2)_3^+ \rightarrow CO_2 + (CO_2)_2^+$ is added to the dissociation energy of CO_2 in the reaction $(CO_2)_2^+ \rightarrow CO_2 + CO_2^+$ (ref 14). An upper bound of 4.9 kcal/mol has been recently reported for the CO_2–cluster bond energy. Alexander, M. L.; Johnson, M. A.; Lineberger, W. C. *J. Chem. Phys.* **1985**, *82*, 5288–5289.

TABLE VIII: Calculated Dissociation Energies (kcal/mol) of $(CO_2)_3^+$ to Monomers

	$(CO_2)_3^+$	
basis set	D_{2h}	C_{3h}
3-21G geometry		
3-21G	31.71	13.68
6-31G	26.55	9.40
6-31G*	17.66	4.86
MP2/6-31G	25.92	12.59
[MP2/6-31G*] (+ZPC//3-21G)	17.03 (16.05)	8.05 (6.54)

(Figure 1). The D_{2h} structure resembles the T-shaped structure with an additional CO_2 molecule added to the opposite side while the C_{3h} structure would permit interactions between oxygens (Figure 1). At all levels the D_{2h} symmetry structure is more stable than the C_{3h} structure (Table VIII). The degenerate electronic state of the C_{3h} complex ($^2E'$) indicates that some stabilization would result as a consequence of a Jahn–Teller distortion.[44] In fact, the C_{3h} structure is not a stationary point at the UHF/3-21G level as nonzero gradients for distortion from C_{3h} symmetry are calculated at the optimized C_{3h} geometry.

The geometry of the D_{2h} $(CO_2)_3^+$ ion complex closely resembles that of the C_{2v} $(CO_2)_2^+$ complex where the O–C interaction has decreased 0.12 Å (2.541 Å → 2.412 Å; 3-21G). The total dissociation is estimated to be 16.0 kcal/mol at the [MP2/6-31G*] + ZPC level (Table VIII), while the dissociation energy for one

(44) Jahn, H. A.; Teller, E. *Proc. R. Soc. London, Ser. A* **1937**, *161*, 220.

CO_2 is calculated to be 4.0 kcal/mol if the dissociation energy of the $(CO_2)_2^+$ complex is determined from the C_{2v} structure at the [MP4SDQ/6-31G*] + ZPC level (12.0 kcal/mol). The experimental values[14] for complete dissociation and dissociation of one CO_2 are 23.0 and 7.4 kcal/mol, respectively. The calculated entropy change of 47.9 cal mol^{-1} K^{-1} is 26.6 cal mol^{-1} K^{-1} greater than the dissociation of one CO_2 from $(CO_2)_2^+$ (Table VII). This value compares favorably with the experimental value[14] of 42.5 cal mol^{-1} K^{-1} for the sum of the first two steps and 23.4 cal mol^{-1} K^{-1} for the entropy change of the second step.

Conclusion

A study has been made of the energetics of clustering in CO_2. The neutral $(CO_2)_2$ complex is more stable in a C_{2h} symmetry structure and is bound by 1.3 kcal/mol. The $(CO_2)_2^+$ ion complex displays two types of binding. In the C_{2v} ion complex the interaction is an ion-induced dipole interaction while the C_{2h} ion complex is bound by a 2-center 3-electron bond. The C_{2h} structure is predicted to be 4.4 kcal/mol more stable but higher levels of correlation could favor the C_{2v} structure relative to the C_{2h} structure. The fact that photoionization and thermodynamic determinations of the dissociation energy disagree may indicate a large geometry change upon ionization. From a comparison of the C_{2h} and the C_{2v} symmetry ion complexes, it is clear that both involve large changes in geometry from the C_{2h} symmetry neutral dimer. Therefore differences in the photoionization and thermodynamic dissociation energies cannot be used to determine which complex is more likely. Higher levels of theory will be required before a definitive prediction can be made for the structure of this ion complex.

The trimer ion is predicted to be of D_{2h} symmetry. The first CO_2 is calculated to be bound by 12.0 kcal/mol while the second CO_2 is bound by 4.0 kcal/mol, which is in reasonable agreement with experimental values corrected to 0 K (15.6 and 7.4 kcal/mol, respectively). The entropy change for dissociation of CO_2 from $(CO_2)_2^+$ is calculated to be 21.3 entropy units while dissociation of one CO_2 from $(CO_2)_3^+$ is 26.6 entropy units.

Acknowledgment. M.L.M thanks the Auburn University Computer Center for a generous allotment of computer time and internal grant 86-71 for financial support. This work was partially support by a grant from the National Science Foundation (CHE83-12505).

An Infrared and Raman Study of the Isotopic Species of α-Quartz

Robert K. Sato* and Paul F. McMillan

Department of Chemistry, Arizona State University, Tempe, Arizona 85287 *(Received: February 9, 1987)*

We have obtained Raman and infrared spectra for the 28/30 Si and 16/18 O isotopic species of α-quartz. The isotopic frequency shifts give valuable information on atomic participation in individual vibrational modes. Comparisons of our isotopic shifts with displacement patterns predicted from a number of dynamical calculations have been made. Most calculated modes agree well with the observed isotope shifts, but some do not. For example, the strong Raman line at 464 cm^{-1} shows no silicon displacement but a large oxygen shift, consistent with its usual assignment to a motion of the bridging oxygens in the plane bisecting the SiOSi linkage. However, the soft mode at 206 cm^{-1}, which is commonly accepted as being due to motion of Si and O around a 3-fold screw axis related to the α-β displacive transition in quartz, shows no Si isotope shift and hence no silicon participation in this vibration.

Introduction

The dynamics of α-quartz have been the subject of considerble experimental and theoretical study. This phase is of particular interest since it forms the simplest crystalline silicate, and also because it shows a displacive phase transition associated with soft phonon behavior to the β-form at 575 °C.[1] In the present study, we have applied the classic technique of isotopic substitution to gain a better understanding of the atomic displacements associated with $k = 0$ vibrational modes in α-quartz.

Quartz is an excellent candidate for an isotopic substitution experiment since there are only two atom types, Si and O, each of which has a stable substitutable isotope, and all of the vibrational modes at $k = 0$ are optically active (species A_1, A_2, and E). In this paper, we report infrared and Raman frequencies for the $^{28}Si^{16}O_2$, $^{28}Si^{18}O_2$, and $^{30}Si^{16}O_2$ isotopic species of quartz.

Experimental Section

The $^{28}Si^{16}O_2$ sample was prepared by gelling $Si(OC_2H_5)_4$ (TEOS) with doubly distilled, deionized H_2O. The gel was fired at 1000 °C for 12 h, and then loaded into a platinum capsule with a trace of ultrapure H_2O. The mix was crystallized hydrothermally at 500 °C and 1 kbar for 1 week in a cold-seal pressure vessel to obtain α-quartz. This was verified by optical microscopy and by Raman spectroscopy. The well-formed, terminated crystals were 20-50 μm in dimension. The ^{28}Si and ^{16}O were present in their natural abundances (92.18 atom % and 99.757 atom %, respectively). Powdered $^{30}SiO_2$ (95.2 atom % ^{30}Si) was purchased from MSD Isotopes. The amorphous material was crystallized hydrothermally at 500 °C and 1 kbar for 1 week to give α-quartz.

The $Si^{18}O_2$ starting material was prepared by hydrolyzing $SiCl_4$ with $H_2{}^{18}O$ (99 atom % ^{18}O), obtained from MSD Isotopes. This was carried out in a drybox under an atmosphere of dry N_2 to avoid contamination with atmospheric oxygen. The $Si^{18}O_2$ powder was then loaded into a platinum capsule with $H_2{}^{18}O$. This sample did not crystallize quartz under the same hydrothermal conditions as the samples above, but consistently gave cristobalite.[2] α-Quartz was obtained by hydrothermal treatment at 400 °C and 4 kbar for 48 h in an internally heated argon gas pressure vessel.

Raman spectra were obtained with an Instruments S.A. U-1000 Raman system, using the 5145-Å line of a Coherent Innova 90-4 argon laser for sample excitation. The microassembly (using 50× and 100× Olympus objectives) was used due to the small sizes of the samples. Laser power at the sample ranged from 5 to 50 mW, and the instrumental slit width was 200 μm, corresponding to a spectral band-pass of near 1.8 cm^{-1}. The absolute wavelength scale of the spectrometer was calibrated against the emission lines of atomic Hg and Ne. Individual spectra in the present study

(1) Sosman, R. B. *The Phases of Silica*; Rutgers University Press: New Brunswick, NJ, 1965.

(2) Carr, R. M.; Fyfe, W. S. *Am. Mineral.* **1958**, *43*, 908.

0022-3654/87/2091-3494$01.50/0 © 1987 American Chemical Society